HAL
open science

Experimental Study of Iron Losses Generated by a Uniform Rotating Field

Alix Bernot, Alexandre Giraud, Yvan Lefèvre, Jean-François Llibre

To cite this version:

Alix Bernot, Alexandre Giraud, Yvan Lefèvre, Jean-François Llibre. Experimental Study of Iron Losses Generated by a Uniform Rotating Field. IEEE Transactions on Magnetics, 2017, 53 (11), pp.6300705. 10.1109/TMAG.2017.2707542 . hal-01652370

HAL Id: hal-01652370

https://hal.science/hal-01652370v1

Submitted on 30 Nov 2017

HAL is a multi-disciplinary open access archive for the deposit and dissemination of scientific research documents, whether they are published or not. The documents may come from teaching and research institutions in France or abroad, or from public or private research centers.

L'archive ouverte pluridisciplinaire **HAL**, est destinée au dépôt et à la diffusion de documents scientifiques de niveau recherche, publiés ou non, émanant des établissements d'enseignement et de recherche français ou étrangers, des laboratoires publics ou privés.

Open Archive TOULOUSE Archive Ouverte (OATAO)
OATAO is an open access repository that collects the work of Toulouse researchers and makes it freely available over the web where possible.

This is an author-deposited version published in : http://oatao.univ-toulouse.fr/
Eprints ID : 19254

To link to this article : DOI:10.1109/TMAG.2017.2707542
URL : http://dx.doi.org/10.1109/TMAG.2017.2707542

To cite this version : Bernot, Alix and Giraud, Alexandre and Lefèvre, Yvan and Llibre, Jean-François *Experimental Study of Iron Losses Generated by a Uniform Rotating Field.* (2017) IEEE Transactions on Magnetics, vol. 53 (n° 11). pp. 6300705. ISSN 0018-9464

Any correspondence concerning this service should be sent to the repository administrator: staff-oatao@listes-diff.inp-toulouse.fr

Experimental Study of Iron Losses Generated by a Uniform Rotating Field

A. Bernot[1], A. Giraud[1,2], Y. Lefèvre[2], and J.-F. Llibre[2]

[1]IRT Saint-Exupéry, 31432 Toulouse, France
[2]Laplace laboratory, University of Toulouse, 31071 Toulouse, France

This paper introduces a mock-up with a solid iron cylinder rotating in a fixed excitation frame powered by dc current. A uniform field is created in the rotating cylinder, which is driven by an external motor. The braking torque is measured, allowing the study of iron losses generated by a uniform rotating field. The aim is to advance toward a vector iron loss model that takes into account different magnetization directions and their interdependency. The eddy current losses are the dominant loss source in the mock-up, rendering it easier to model. A standard eddy currents model is proposed. It models well the losses at low and medium magnetic flux density, but lower losses are measured near saturation levels. This could be due to the high thickness to radius ratio changing the eddy current paths near the edges of the rotor, which can be later analyzed by a full 3-D finite-element method analysis. A 2-D finite-element method simulation is performed, which estimates the magnetic flux heterogeneity in the rotor. Several lessons are drawn from this mock-up, which prepares a second version with a higher speed and a longer laminated stack rotor. A higher air gap will decrease the voltage fluctuation in the primary winding, a smaller angular opening of the excitation frame will improve the uniformity of the flux in the rotor.

***Index Terms*—Eddy currents, iron losses, rotating field, rotational losses.**

I. Introduction

IRON losses in electric machines have been studied for decades [1], [2]. Following the introduction of power electronics drives, the speed and base frequencies of electric machines increased. This allowed a volume reduction at constant power, because the size of a motor is essentially linked to its torque [3]. With higher base frequencies, the iron losses have become the dominant loss source in many electric machines [4], [5], enhancing the need for accurate iron loss modeling [6].

Traditional iron loss measurements of soft magnetic materials are done on Epstein frames with loose lamination stacks, with a sinusoidal magnetic flux density, according to the IEC 60404-2 norm. Several iron loss models, such as the widespread Bertotti model [7], have been developed to predict losses in an Epstein frame. These models are 1-D, modeling only a non-rotating uniform field. They also model only one single sine frequency, and do not take into account the influence of the spectrum of the magnetic flux density.

Several models have tried to bypass these limits. The Preisach and Play models, which are equivalent, model the quasi-static hysteresis, accurately taking into account the field waveforms [8], but it remains a scalar 1-D model. The loss-surface model relies on a mapping of the losses, dynamically linking different points of a static loss surface. However, this model is also a scalar model, which poorly takes into account the influence of a variable direction magnetic field.

This study is a first step toward a model of variable direction magnetic field iron losses, which will lead later to a full 2-D iron losses model. One of the aims of such a model is to accurately take into account the interdependence of the magnetization directions. For instance, if a strong magnetic field is applied in a direction called x, the relative permeability of the steel sheet in the orthogonal y-direction will be small because of saturation, which can lead to higher losses.

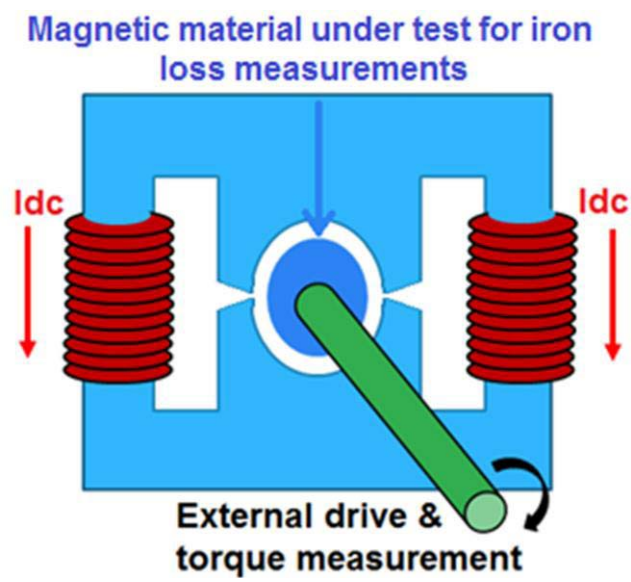

Fig. 1. Mock-up synopsis.

The study presented in this paper is an experimental study. The results will give a first insight into the validity of the models. It will also help to assess the difficulties of setting up a more complete experiment.

II. Experiment Description

A. Mock-Up Description

The mock-up is fundamentally an eddy current brake. A solid cylinder is rotating inside a two-pole magnetization frame, as presented in Figs. 1 and 2.

The aim of the magnetizing frame is to produce a constant uniform vertical magnetic field inside the rotating cylinder. Its two windings have 375 turns each, with a copper section of 10 mm^2. They are supplied with the same regulated dc

Digital Object Identifier 10.1109/TMAG.2017.2707542

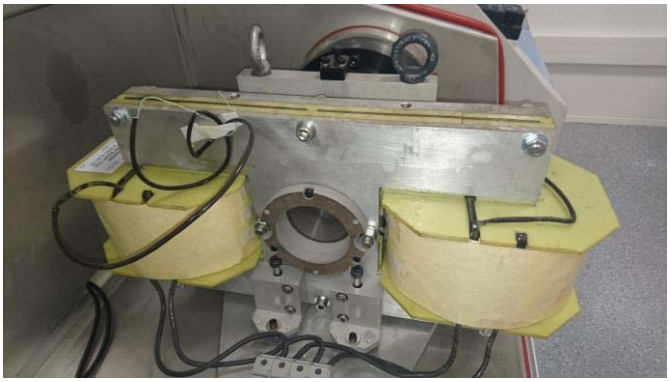

Fig. 2. Mock-up mounted in the test bench.

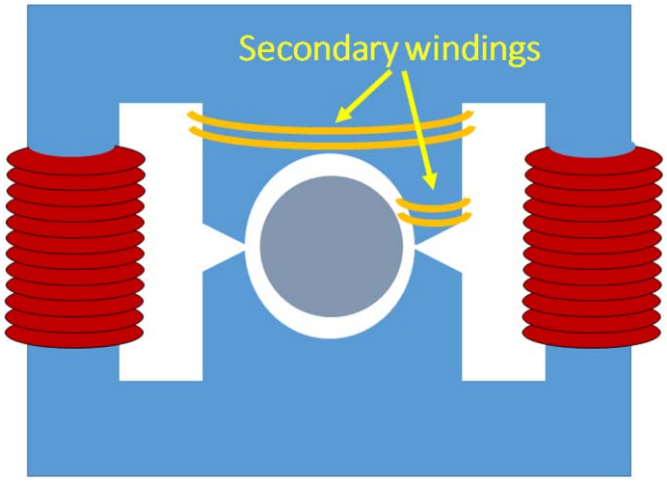

Fig. 3. Secondary coils.

current generated by a lab regulated power supply. The stator magnetic circuit is composed of 0.2 mm non-oriented silicon-steel (NO20) in order to ensure low stator iron losses. The magnetic flux in the stator will be roughly constant, which will also limit the stator iron losses.

The sample under test is a solid pure iron cylinder with an 80 mm outer diameter and a 5 mm axial thickness. It is glued onto a non-magnetic shaft to minimize flux leakage and preserve the magnetic shape. The shaft is mounted on air bearings in order to minimize friction losses. It is driven by an external motor through a torque meter, and the resistant torque is measured. This torque is mainly composed of the iron losses in the rotor. The high thickness without lamination will generate high eddy currents and therefore high iron losses, which will be easier to measure. Lower speeds are required to reach significant torque, which eases mechanical conception and rotor balancing requirements. The rotor is balanced for 3000 rpm (50 Hz). A similar second mock-up with a lamination stack sample rotating at higher speed (40 000 rpm) is planned for later. It will have much smaller resistant torque and will require greater care for the driveline design, so that the mechanical losses remain much smaller than the iron losses. The lessons drawn from this simpler mock-up will help design and make the second version.

Two secondary coils are added around the center of the stator magnetic circuit (Fig. 3). Made of thin magnet wire, their aim is to measure the magnetic flux crossing the rotor. When steady state is reached, the current supplied in the primary windings is reversed thanks to two solid state switches. The voltage generated in the secondary coils is measured, stored, and integrated. Applying the Lenz law (1), this gives the total magnetic flux crossing the center of the stator φ_1 and the leakage flux bypassing the rotor φ_2. Δt is the switching time (current rise time), V is the voltage over the secondary coil, and N is the number of turns

$$\varphi = \int_{\Delta t} \frac{V}{N} \cdot dt. \tag{1}$$

Installing a secondary coil directly around the rotor was too difficult, so the choice was made to measure both total and leakage flux. It is assumed the leakage flux is symmetric, so only one secondary leakage coil is installed.

TABLE I
AVERAGE PRIMARY WINDING VOLTAGES (V)

Current (A)	At 0rpm	Minimum	Maximum
1	0.153	0.1492	0.1537
5	0.7304	0.7293	0.7325
18	2.6576	2.6576	2.6686

B. Experiment Setup

The stator is supplied with a regulated dc current between 0 and 60 A. The driving motor is controlled with a constant speed between 0 and 3000 rpm. The torque is measured with a T40 contactless HBM torquemeter. At each speed, a torque measurement is first made without current, and is then subtracted from the other measurements with current. This no-current torque measurement is due to both the torquemeter offset and the mechanical losses. This subtraction helps to ensure that the considered torque is only due to the iron losses. The voltage in the primary windings is monitored in order to verify the power flows. If the voltage measured is only due to the Joule losses of the windings, this will ensure that all the iron losses are measured by the mechanical torque and that no power escapes through the primary windings.

At a given current, once the steady state is reached, the current is reversed and the voltage in the secondary coils is measured and stored.

III. RESULTS

A. Primary Voltage

The voltage powering the primary winding has been measured at each speed and primary current, its time average calculated and compared to the Joule voltage drop. For each current, the Joule losses were determined by supplying the primary winding with the rotor stationary. They were always measured before and after the experiment, to check for the temperature rise of the winding, which would increase the losses. Table I presents the average primary voltages measured with the all-speed minimum and maximum measured (that is, in the list of the primary voltage measured at different speeds and a given current, the minimum and the maximum voltage are extracted and listed in Table I).

The average voltage appears to be independent of the speed and equal to the Joule voltage drop. The measured fluctuations are below the probe's accuracy. This result proves that no mechanical power is passed to the primary winding,

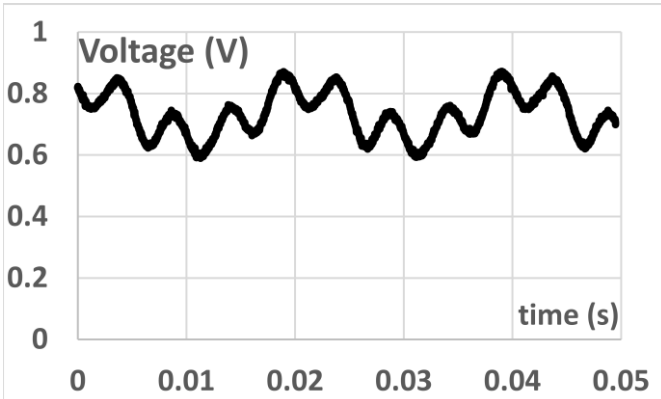

Fig. 4. Primary voltage at 3000 rpm and 5 A (3750 At).

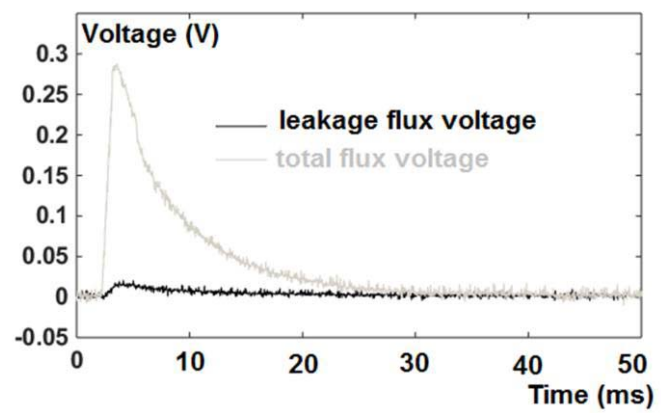

Fig. 5. Secondary voltage after current switching at 3000 rpm and 1 A.

and so all the iron losses are retrieved in the mechanical torque (alongside the mechanical losses).

On the other hand, as can be seen in Fig. 4, there is a significant oscillation with a peak-to-peak value worth 30% of the voltage mean (equal to the Joule voltage drop), with a time period equal to the mechanical period. This oscillation can be due to the mechanical imperfection of the rotating cylinder, with variations of the air gap leading to a reluctance variation of the magnetic circuit. The mechanical precision of the rotating cylinder is 0.1 mm, and the air gap is 0.3 mm, which may indeed lead to a 30% air gap fluctuation ($\pm$0.1 mm), and a 30% reluctance variation. In order to reduce this effect, the next version of the mock-up can have a bigger air gap in order to limit the relative air gap variations.

B. Magnetic Flux Density

The magnetic flux density is measured at different currents and speeds by inverting the current in the primary winding and integrating the voltage measured over the secondary coils. The integration window is manually determined for each measurement based on the primary current. Fig. 5 shows the measured voltage at 1 A (primary winding current) and 100 rpm, with total flux winding in gray and leakage flux winding in black. The measurement is precise enough to be exploited. The magnetic flux density in this case, calculated by means of voltage integration is 0.336 T. The leakage flux is 22% of the total measured flux (the secondary winding for total flux

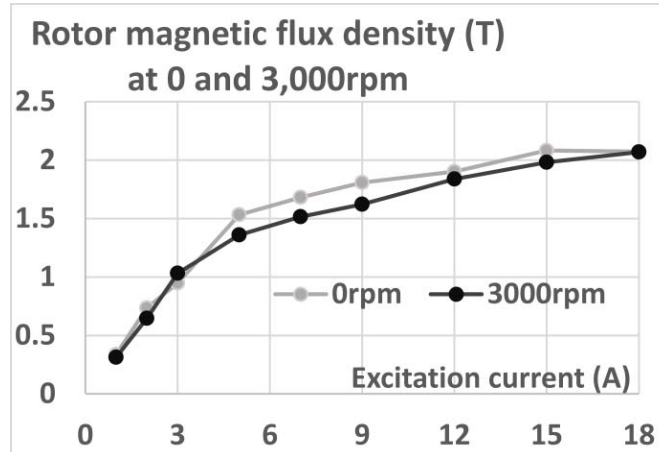

Fig. 6. Rotor magnetic flux density at 0 and 3000 rpm.

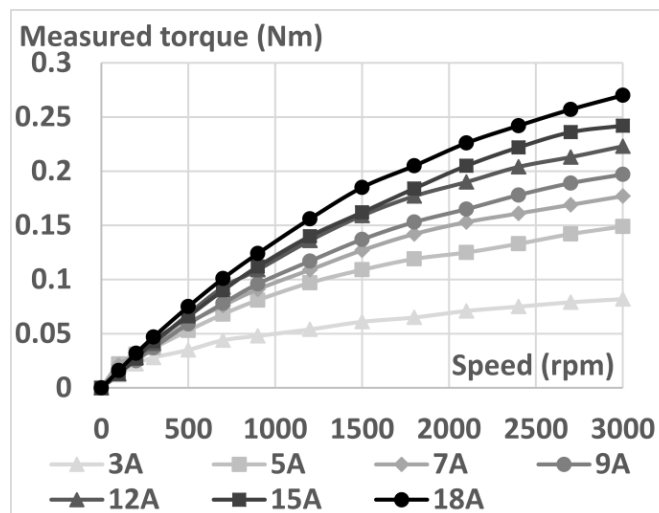

Fig. 7. Measured torque at different excitation currents.

has five turns, and the secondary winding for leakage flux has three turns).

At constant excitation current, the magnetic flux density inside the sample will decrease when the speed increases, because of the eddy currents inside the sample. This has to be taken into account in the model. The maximum measured average magnetic flux density drop between 0 and 3000 rpm is 11%, as can be seen in Fig. 6.

C. Torque

The torque is measured for several excitation currents and speed. The measurements are presented in Fig. 7.

A least squares $A \cdot \Omega^B$ correlation of the torque is done at each current. The average correlated exponent (B) is 0.7. It is to be compared with the iron losses models.

IV. Modeling and Simulation

A. Power Balance

The system has two power sources, the driving motor supplying mechanical energy and the stator windings supplying electrical energy. It can dissipate power through friction (mechanical losses), eddy current Joule losses in the

rotor (along with other iron losses such as hysteresis losses), Joule losses in the stator winding, and induction in the stator winding (Lenz's law) passing to the regulated power supply.

It is assumed that the mechanical losses depend only on the speed of the system, and depend neither on its torque nor on its magnetism. At a given speed, the driving torque without excitation current allows us to identify the mechanical losses. They will be subtracted from the torque measured with excitation current, which leaves only the electromagnetic effects.

The variable magnetic flux in the rotor induces eddy currents, which in turn create Laplace forces. The work of these forces is the electromagnetic braking torque, which is equal to the total braking torque minus the braking torque at the same speed without primary current. The work of these forces can either be converted into Joule losses in the rotor, or passed to the primary winding (which is the case for instance with a solid rotor induction machine) [10]. The power flowthrough the primary winding was measured to be exactly the Joule losses in the stator, which means no mechanical power is passed to the stator winding. Finally, it is concluded that the electromagnetic torque fully corresponds to the iron losses in the rotor.

B. Bertotti Eddy Current Model

The main iron loss source in solid metal is eddy currents. The usual model for iron losses is detailed by Bertotti [7]. It models the iron losses with a thin sheet model, assuming the magnetic flux density is uniform and sinusoidal. The skin effect is neglected, since the frequency is low (50 Hz maximum). The iron loss power density is given by

$$P = \frac{\pi^2}{6} \frac{e^2 \cdot B_{\max}^2 \cdot f^2}{\rho} \tag{2}$$

where $B_{\max}$ is the peak magnetic flux density, e is the sheet thickness (5 mm), f is the frequency, and ρ is the resistivity (1×10^{-7} Ω·m).

A uniform magnetic flux density in the mock-up rotor is considered. With a constant speed, the magnetic flux density at a point on the rotor will be sinusoidal, so the Bertotti model can be used. The total iron losses in the rotor are calculated with this model at 3000 rpm, and compared with the mechanical power losses measured (electromagnetic braking only, the mechanical friction measured without current having been subtracted) measured in Fig. 8.

The simple eddy current model is rather accurate, except at higher magnetic flux densities (above 1.8 T, near saturation), where it begins to overestimate. The higher the magnetic flux density, the more the eddy currents are the dominant phenomenon. At saturation levels, there should be neither hysteresis nor excess losses because there is no magnetic domain, so no Bloch wall movement [11], [12]. The magnetic flux density has a constant module and a rotating direction, so under saturation conditions, whatever the direction of the magnetic flux, there is only one large magnetic domain and indeed no wall movement. The iron losses should then be proportional to the square of the magnetic flux density (iron loss formula), because the eddy currents are the only loss source left.

The missing losses at high magnetic flux density could be due to a modification of the eddy current paths due to the lower relative permeability at saturation. This can be later investigated in detail with 3-D finite-elements analysis. The considered eddy current model assumes the sheet is thin, and neglects the changing current paths around the edges and the skin effect. The ratio between the rotor radius and thickness is 0.125, which is not that small and may have to be taken into account at higher magnetic flux densities. In an electric machine, such width to thickness ratio can be found in some parts of the machine, for instance a 3 mm tooth with a 0.35 mm laminated sheet, so it is interesting to investigate further.

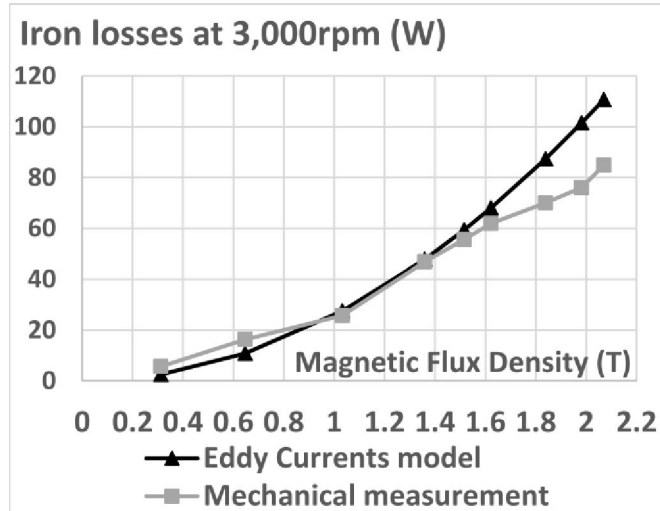

Fig. 8. Modeled iron losses.

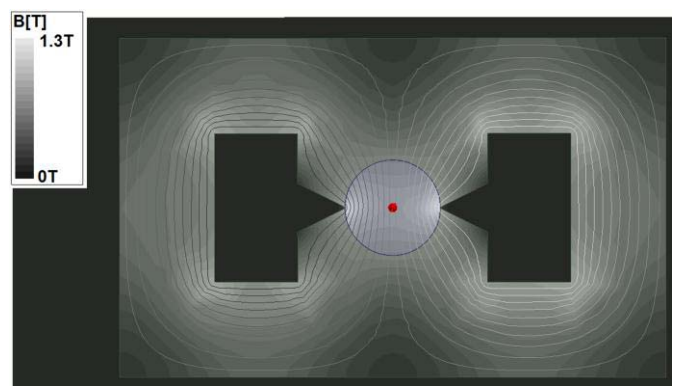

Fig. 9. Overall magnetic flux density with a 1 T rotor average.

C. Finite-Element Method Model

The mock-up is simulated with Ansys Maxwell with 2-D finite-element method. NO20 and pure iron are modeled thanks to anhysteretic $B(H)$ magnetization curves. The eddy currents are not modeled for the computation of the magnetic flux density.

The magnetic flux density in the rotor is not very homogeneous, with a 40% peak-to-peak fluctuation of the module, as can be seen in Fig. 9. 75% of this fluctuation is concentrated at the left and right edges of the rotor, with also an important deviation of the flux direction there. This is monitored by plotting the radial and tangential components of the magnetic flux density along circles of several radii, as shown in Fig. 10. It will be improved in the next version of the mock-up, by reducing the angular opening of the stator, in order to

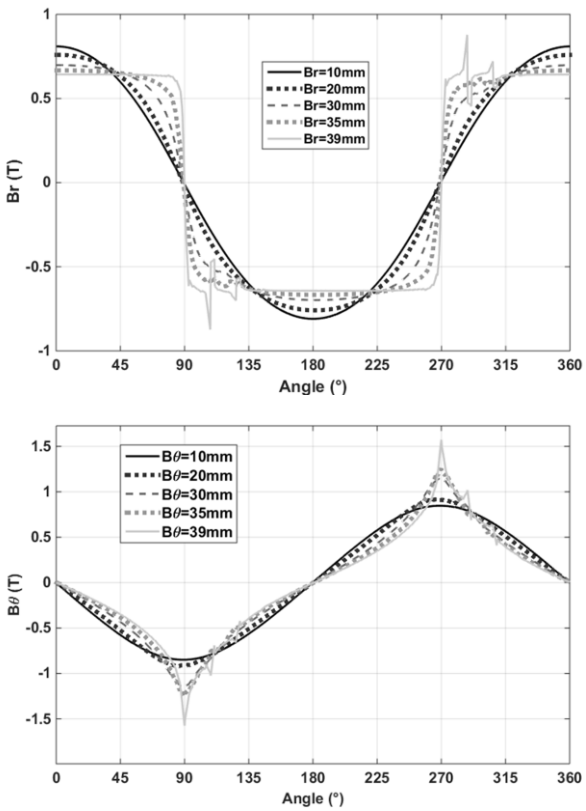

Fig. 10. Radial and tangential magnetic flux densities in the rotor.

reduce this flux concentration effect. The optimum stator shape that maximizes the flux homogeneity in the rotor can be studied with a finite-element method simulation.

Around the center, below a 20 mm radius, the magnetic flux density is uniform, and its radial and tangential components are sinusoidal. Closer to the edge, above a 30 mm radius, the magnetic flux density is much more disturbed. This phenomenon could be a part of the cause of the iron loss drop at higher magnetic flux densities.

V. Conclusion

A mock-up of a rotating cylinder in a uniform magnetic field has been built and tested. Its aim is to study the losses of a constant rotating field. This will help developing a vector iron loss model, which really takes into account the interdependency of the magnetization directions.

This mock-up is a lower cost first step toward a more complex one, which will be faster and have a sheet stack rotor. Its rotor is solid iron, in order to increase iron losses and improve their measurability. It does not require complex rotor balancing because it rotates at only 3000 rpm. Several lessons have been drawn in order to prepare the final version. The small air gap induces an important reluctance fluctuation, inducing a large voltage variation in the primary winding. This effect can be reduced by increasing the air gap; the final version can have an air gap of up to 1 mm. The main drawback of a larger air gap is the need for higher excitation currents to reach high magnetic flux densities, but the mock-up was not pushed to its limits (the current density in the primary winding was 2 A/mm^2 at 2 T). The measurement of the magnetic flux by means of secondary windings and current inversion was satisfactory and will be kept. Finally, the magnetic flux density in the rotor was not homogeneous. This can be improved in the next mock-up by a careful study of the stator magnetic circuit. Particularly, the angular opening of the stator directly circling the rotor may be reduced to limit the flux concentration at the left and right edges of the rotor.

Regarding the measured results, the iron losses at low and medium magnetic flux densities can be accurately modeled by a traditional eddy currents model. However, iron losses are lower than expected at higher speeds and higher magnetic flux densities. This could be due to the high thickness to radius ratio, which limits the validity of the thin sheet eddy current model, with different eddy current paths around the edges. This effect might be strengthened near saturation levels because of the low relative permeability. A complete 3-D eddy currents analysis by means of finite-element method simulation would help confirm this hypothesis. These results confirm the need for the development of higher vector iron loss models, which fully take into account different magnetization directions and their interdependency.

References

[1] C. P. Steinmetz, "On the law of hysteresis (part III.), and the theory of ferric inductances," presented at the 11th General Meeting Amer. Inst. Electr. Eng., Philadelphia, PA, USA, May 1894.

[2] C. D. Graham, Jr., "Physical origin of losses in conducting ferromagnetic materials (invited)," *J. Appl. Phys.*, vol. 53, no. 11, p. 8276, 1982.

[3] A. Boglietti, A. Cavagnino, M. Lazzari, and S. Vaschetto, "Preliminary induction motor electromagnetic sizing based on a geometrical approach," *IET Electr. Power Appl.*, vol. 6, no. 9, pp. 583–592, 2012.

[4] A. Krings, J. Soulard, and O. Wallmark, "PWM influence on the iron losses and characteristics of a slotless permanent-magnet motor with SiFe and NiFe stator cores," *IEEE Trans. Ind. Appl.*, vol. 51, no. 2, pp. 1475–1484, Mar./Apr. 2015.

[5] M. van der Geest, H. Polinder, and J. A. Ferreira, "Influence of PWM switching frequency on the losses in PM machines," presented at the Int. Conf. Elect. Mach. (ICEM), Berlin, Germany, 2014.

[6] K. Yamazaki and N. Fukushima, "Iron loss model for rotating machines using direct eddy current analysis in electrical steel sheets," *IEEE Trans. Energy Convers.*, vol. 25, no. 3, pp. 633–641, Sep. 2010.

[7] G. Bertotti, "General properties of power losses in soft ferromagnetic materials," *IEEE Trans. Magn.*, vol. 24, no. 1, pp. 621–630, Jan. 1988.

[8] O. de la Barrière, H. B. Ahmed, M. Gabsi, and M. LoBue, "Computation of the losses in a laminated ferromagnetic material under bidirectional induction excitation," *IEEE Trans. Magn.*, vol. 46, no. 2, pp. 610–613, Feb. 2010.

[9] A. Frias, A. Kedous-Lebouc, C. Chillet, L. Albrt, and L. Calegari, "Electrical steel solicitation in traction electrical machine," in *Proc. 38th Annu. Conf. IEEE Ind. Electron. Soc. IECON*, Montreal, QC, Canada, Oct. 2012, pp. 1770–1774.

[10] O. Bottauscio, M. Chiampi, and A. Manzin, "Modeling analysis of the electromagnetic braking action on rotating solid cylinders," *Appl. Math. Model.*, vol. 32, no. 1, pp. 12–27, 2008.

[11] S. Tumanski, *Handbook of Magnetic Measurements*. Boca Raton, FL, USA: CRC Press, 2011.

[12] K. Overshott, "The use of domain observations in understanding and improving the magnetic properties of transformer steels," *IEEE Trans. Magn.*, vol. 12, no. 6, pp. 840–845, Nov. 1976.